

Terphenyl Ligand Stabilized Lead(II) Derivatives: Steric Effects and Lead–Lead Bonding in Diplumbenes

Shirley Hino, Marilyn Olmstead, Andrew D. Phillips, Robert J. Wright, and Philip P. Power*

Department of Chemistry, University of California, Davis, One Shields Avenue, Davis, California 95616

Received June 24, 2004

The reaction of PbBr_2 with the lithium reagents $\text{LiC}_6\text{H}_3\text{-2,6-(C}_6\text{H}_3\text{-2,6-Pr}^i\text{)}_2$ (LiArPr_2) and $\text{Et}_2\text{O}\cdot\text{LiC}_6\text{H}_3\text{-2,6-(2,6-Pr}^i\text{-4-Bu}^t\text{C}_6\text{H}_2)_2$ ($\text{Et}_2\text{O}\cdot\text{LiArPr}_2\text{Bu}^t$) furnished the bromide bridged organolead(II) halides $\{\text{Pb}(\mu\text{-Br)ArPr}_2\}_2$ (**1**) and $\{\text{Pb}(\mu\text{-Br)ArPr}_2\text{Bu}^t\}_2$ (**2**) as orange crystals. Treatment of **1** with a stoichiometric amount of methylmagnesium bromide resulted in the “diplumbene” $\text{Pr}_2\text{Ar(Me)PbPb(Me)ArPr}_2$ (**3**). The addition of 1 equiv of 4-*tert*-butylphenylmagnesium bromide to **1** afforded the feebly associated, Pb–Pb bonded species $\{\text{Pb}(\text{C}_6\text{H}_4\text{-4-Bu}^t)\text{ArPr}_2\}_2$ (**4**), whereas the corresponding reaction of *tert*-butylmagnesium chloride and **1** afforded the monomer $\text{Pb}(\text{Bu}^t)\text{ArPr}_2$ (**5**). The reaction of the more crowded aryl lead(II) bromide $\{\text{Pb}(\mu\text{-Br)ArPr}_3\}_2$ ($\text{Ar}^* = \text{C}_6\text{H}_3\text{-2,6(C}_6\text{H}_2\text{-2,4,6-Pr}^i\text{)}_2$) with 4-isopropylbenzylmagnesium bromide or $\text{LiSi}(\text{SiMe}_3)_3$ yielded the monomers **6**, $[\text{Pb}(\text{CH}_2\text{C}_6\text{H}_4\text{-4-Pr}^i)\text{ArPr}_3]$, or **7**, $[\text{Pb}(\text{Si}(\text{SiMe}_3)_3)\text{ArPr}_3]$. All compounds were characterized with use of X-ray crystallography, ^1H , ^{13}C , and ^{207}Pb NMR (**3–7**), and UV–vis spectroscopy. The dimeric Pb–Pb bonded ($\text{Pb–Pb} = 3.1601(6) \text{ \AA}$) structure of **3** may be contrasted with the previously reported monomeric structure of $\text{Pb}(\text{Me})\text{ArPr}_3$, which differs from **3** only in that it has para Prⁱ substituents on the flanking aryl rings. The presence of these groups is sufficient to prevent the weak Pb–Pb bonding seen in **3**. The dimer **4** displays a Pb–Pb distance of $3.947(1) \text{ \AA}$, which indicates a very weak lead–lead interaction, and it is possible that this close approach could be caused by packing effects. The monomeric structures of **6** and **7** are attributable to steric effects and, in particular, to the large size of ArPr_3 .

Introduction

Since their discovery in the 1970s, diorganolead(II) compounds, PbR_2 ,¹ ($\text{R} =$ variety of bulky groups) have received less attention than the corresponding silicon,^{2,3} germanium,^{3–6} and tin^{6–8} species. Currently, ca. 40 examples are known. They exist mainly as PbR_2 , monomers,^{6,8} weakly

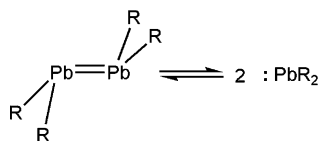
bonded dimers, R_2PbPbR_2 ,^{8,9} or as a trimer $(\text{PbR}_2)_3$,¹⁰ which features a unique Pb_3 ring. The lead–lead bonding in the “diplumbene” dimers, R_2PbPbR_2 , is of considerable relevance to the debate on multiple bonding in the heavier main group

* To whom correspondence should be addressed. E-mail: pppower@ucdavis.edu.

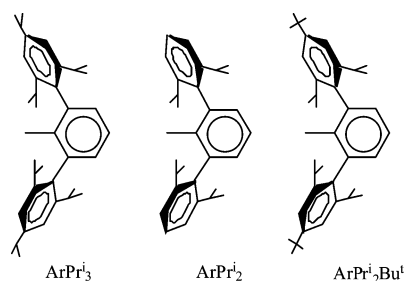
- (1) (a) Davidson, P. J.; Lappert, M. F. *Chem. Commun.* **1973**, 317. (b) Davidson, P. J.; Harris, D. H.; Lappert, M. F. *J. Chem. Soc., Dalton Trans.* **1976**, 21, 2268. (c) Cotton, J. D.; Davidson, P. J.; Lappert, M. F. *J. Chem. Soc., Dalton Trans.* **1976**, 21, 2275.
- (2) (a) West, R.; Fink, M. J.; Michl, J. *Science (Washington, D.C.)* **1981**, 214, 2343. (b) Weidenbruch, M. *J. Organomet. Chem.* **2002**, 646, 39. (c) West, R. *Polyhedron* **2002**, 21, 467. (d) Okazaki, R.; West, R. *Advances in Organometallic Chemistry* **1996**, 39, 231. (e) Weidenbruch, M. In *Chemistry of Organic Silicon Chemistry*; Rappoport, Z., Apeloig, Y., Ed.; Wiley: Chichester, 2001; Vol. 3, Chapter 5. (f) Apeloig, Y.; Karni, M.; Muller, T. In *Organosilicon Chemistry II: From Molecules to Materials*; Auner, N., Weis, J., Eds.; VCH: Weinheim, 1996; p 263.
- (3) (a) Weidenbruch, M. *Organometallics*, **2003**, 22, 4348. (b) Tokitoh, N.; Okazaki, R. *Coord. Chem. Rev.* **2000**, 210, 251–277. (c) Weidenbruch, M. *Eur. J. Inorg. Chem.* **1999**, 3, 373. (d) Power, P. P. *Chem. Rev.* **1999**, 99, 3463.

- (4) Tokitoh, N.; Kishikawa, K.; Okazaki, R.; Sasamori, T.; Nakata, N.; Nobuhiro, T. *Polyhedron*, **2002**, 21, 563.
- (5) (a) Barrau, J.; Escudie, J.; Satge, J. *Chem. Rev.* **1990**, 90, 283. (b) Barrau, J.; Rima, G. *Coord. Chem. Rev.* **1998**, 178–180, 593.
- (6) (a) Klinkhammer, K. W. In *Chemistry of Organic Germanium, Tin and Lead Compounds*; Rappoport, Z., Ed.; Wiley: Chichester, 2002; Vol. 2, Part 1, Chapter 4. (b) Tokitoh, N.; Okazaki, R. In *Chemistry of Organic Germanium, Tin and Lead Compounds*; Rappoport, Z., Ed.; Wiley: Chichester, 2002; Vol. 2, Part 1, Chapter 13. (c) Weidenbruch, M. *Main Group Met. Chem.* **2001**, 24, 621–631.
- (7) (a) Eichler, B. E.; Phillips, A. D.; Power, P. P. *Organometallics* **2003**, 22, 5423. (b) Eichler, B. E.; Power, P. P. *Inorg. Chem.* **2000**, 39, 5444.
- (8) Klinkhammer, K. *Polyhedron* **2002**, 21, 587.
- (9) (a) Klinkhammer, K. W.; Fässler, T. F.; Grützmacher, H. *Angew. Chem., Int. Ed.* **1998**, 37, 124. (b) Sturmman, M.; Weidenbruch, M.; Klinkhammer, K. W.; Lissner, F.; Marsmann, H. *Organometallics* **1998**, 17, 4425. (c) Sturmman, M.; Saak, W.; Marsmann, H.; Weidenbruch, M. *Angew. Chem., Int. Ed.* **1999**, 38, 187–189. (d) Sturmman, M.; Saak, W.; Weidenbruch, M. *Z. Anorg. Allg. Chem.* **1999**, 625, 705. (e) Stuermann, M.; Saak, W.; Weidenbruch, M.; Klinkhammer, K. W. *Eur. J. Inorg. Chem.* **1999**, 4, 579.
- (10) Stabenow, F.; Saak, W.; Marsmann, H.; Weidenbruch, M. *J. Am. Chem. Soc.* **2003**, 125, 10172.

elements, since they comprise, along with the neighboring dibismuthenes¹¹ (RBI=BiR), the heaviest homonuclear multiple bonds. However, the divalent lead compounds differ from their bismuth counterparts in that they generally dissociate in solution according to the following equilibrium:



Furthermore, the observed lead–lead bond distances^{8,9} (2.903–3.527 Å) are generally longer than single bonds in tetravalent diplumbanes, R₃PbPbR₃, which range from ca. 2.84 to 2.97 Å.¹² Their tendency to dissociate and the long Pb–Pb distances indicate weak metal–metal bonding. This is a consequence of the requirement to use very stable 6s electrons in bonding if a full fledged Pb–Pb double bond is to be observed. We have previously shown that terphenyls are useful ligands for the stabilization of a variety of low valent and multiply bonded group 14 species.¹³ In the case of lead, simple monomers of formula Pb(R)ArPr₃ (R = Me, Ph, Bu^t; ArPr₃ = –C₆H₃-2,6-(2,4,6-C₆H₂-Pr₃)₂)¹⁴ have been prepared and characterized. Also, the ArPr₃ ligand has been used in the isolation of a “diplumbyne”,¹⁵ Pr₃ArPbPbArPr₃, which has a long single Pb–Pb 3.1881(1) Å bond rather than a triple one. The stabilization of these molecules results from the protecting character of the ArPr₃ ligand (see graphic), which carries flanking aryl rings that have isopropyl substituents at the ortho and para positions. We now show that elimination of the para substituents of the flanking rings, to give the slightly less crowded ligand ArPr₂ (ArPr₂ = –C₆H₃-2,6(2,6-C₆H₃-Pr₂)₂), enables a dimeric diplumbene compound Pr₂Ar(Me)PbPb(Me)ArPr₂ to be observed. In addition, the effects of altering the coligands on the structure and spectroscopy of the compounds are described.



- (11) (a) Tokitoh, N.; Arai, Y.; Sasamori, T.; Okazaki, R.; Nagase, S.; Uekusa, H.; Ohashi, Y. *J. Am. Chem. Soc.* **1998**, *120*, 433. (b) Tokitoh, N.; Arai, Y.; Okazaki, R.; Nagase, S. *Science* **1997**, *277*, 78.
- (12) (a) Mallela, S. P.; Geanangel, R. A. *Inorg. Chem.* **1994**, *33*, 6357. (b) Whittaker, S. M.; Cervantes-Lee, F.; Pannell, K. H. *Inorg. Chem.* **1994**, *33*, 6406–8. (c) Mallela, S. P.; Myrczek, J.; Bernal, I.; Geanangel, R. A. *J. Chem. Soc., Dalton Trans.* **1993**, *19*, 2891. (d) Shibata, K.; Tokitoh, N.; Okazaki, R. *Tetrahedron Lett.* **1993**, *34*, 1499. (e) Okazaki, R.; Shibata, K.; Tokitoh, N. *Tetrahedron Lett.* **1991**, *32*, 6601. (f) Kleiner, N.; Draeger, M. Polyplumbanes. I. *J. Organomet. Chem.* **1985**, *293*, 323.
- (13) (a) Twamley, B.; Haubrich, S. T.; Power, P. P. *Adv. Organomet. Chem.* **1999**, *44*, 1–65. (b) Clyburne, J. A. C.; McMullen, N. *Coord. Chem. Rev.* **2000**, *210*, 73–99.
- (14) Pu, L.; Twamley, B.; Power, P. P. *Organometallics* **2000**, *19*, 2874.
- (15) Pu, L.; Twamley, B.; Power, P. P. *J. Am. Chem. Soc.* **2000**, *122*, 3524.

Experimental Section

General Procedures. All manipulations were carried out by using modified Schlenk techniques under an argon atmosphere or in a Vacuum Atmospheres HE-43 drybox. All solvents were distilled from Na/K alloy and degassed twice before use. The lithium aryls and silyls, LiArPr₂,¹⁶ Pr₃ArLi·OEt₂,¹⁶ Bu^tPr₂ArLi·OEt₂,¹⁷ and LiSi(SiMe₃)₃,¹⁸ were prepared according to literature procedures. The compounds PbBr₂, CH₃MgBr (3.0 M in Et₂O), and Bu^tMgCl (20 wt % in THF) were purchased commercially and used as received. 4-Prⁱ-C₆H₄-CH₂MgBr and 4-Bu^t-C₆H₄MgBr were freshly prepared prior to use. ¹H, ¹³C, and ²⁰⁷Pb NMR data were recorded on a Varian 300 MHz or Varian 400 MHz instrument and referenced to the deuterated solvent and 1 M Pb(NO₃)₂ in D₂O.¹⁹

{Pb(μ-Br)ArPr₂}₂, 1. The lithium aryl LiArPr₂ (4.805 g, 11.88 mmol) was dissolved in diethyl ether (45 mL), and the solution was added dropwise over 40 min to a suspension of PbBr₂ (4.73 g, 12.88 mmol) in diethyl ether (10 mL) with cooling in an ice bath. The solution was allowed to warm to room temperature and stirred overnight. The diethyl ether was removed under reduced pressure, and the orange solid was extracted with toluene (100 mL) and filtered through Celite. The orange filtrate was concentrated to incipient crystallization (ca. 20 mL) and stored in a ca. –20 °C freezer to afford **1** as orange crystals. Yield: 5.70 g, 70%. Mp: 201–206 °C. Anal. Calcd for C₃₀H₃BrPb: C, 52.62; H, 5.45. Found: C, 51.88, H, 5.52. ¹H NMR (C₆D₆): δ 1.02 (d, 12H, o-CH(CH₃)₂) ³J_{HH} = 6.60 Hz; 1.34 (d, 12H, o-CH(CH₃)₂) ³J_{HH} = 6.90 Hz; 3.09 (sept, 4H, o-CH(CH₃)₂) ³J_{HH} = 6.90 Hz; 7.13 (d, 4H, m-C₆H₃Pr₂) ³J_{HH} = 2.10 Hz; 7.22 (t, 2H, p-C₆H₃Pr₂) ³J_{HH} = 6.00 Hz; 7.28 (t, 1H, p-C₆H₃) ³J_{HH} = 6.00 Hz; 7.91 (d, 2H, m-C₆H₃) ³J_{HH} = 4.80 Hz. ¹³C{¹H} NMR (C₆D₆): δ 23.74 (o-CH(CH₃)₂); 26.28 (o-CH(CH₃)₂); 30.77 (o-CH(CH₃)₂); 123.52 (m-C₆H₃Pr₂); 125.59 (p-C₆H₃); 138.80 (i-C₆H₃Pr₂); 145.63 (p-C₆H₃Pr₂); 147.80 (o-C₆H₃Pr₂); 147.85 (o-C₆H₃); 286.77 (i-C₆H₃). UV–vis (hexane): λ_{max} 416.0 nm, ε 740 M^{–1} cm^{–1}.

{Pb(μ-Br)ArPr₂Bu^t}₂, 2. In a similar manner, the reagent ArPr₂·OEt₂ (1.35 g, 2.28 mmol) was reacted with PbBr₂ (1.20 g, 3.25 mmol). Workup, as described for **1**, afforded **2** as orange crystals. Yield: 1.00 g, 55%. Mp: 250–256 °C. ¹H NMR (C₆D₆): δ 1.11 (d, 12H, o-CH(CH₃)₂) ³J_{HH} = 6.80 Hz; 1.37 (d, 12H, o-CH(CH₃)₂) ³J_{HH} = 6.80 Hz; 1.38 (s, 18H, C(CH₃)₃); 3.16 (sept, 4H, o-CH(CH₃)₂) ³J_{HH} = 6.80 Hz; 7.32 (s, 1H, p-C₆H₃) ³J_{HH} = 7.2 Hz; 7.36 (s, 4H, m-C₆H₂Pr₂Bu^t); 8.03 (d, 2H, m-C₆H₃) ³J_{HH} = 7.2 Hz. ¹³C{¹H} NMR (C₆D₆): δ 23.79 (o-CH(CH₃)₂); 26.52 (o-CH(CH₃)₂); 30.93 (o-CH(CH₃)₂); 31.74 (C(CH₃)₃); 35.10 (C(CH₃)₃); 119.20 (m-C₆H₂Pr₂Bu^t); 120.04 (m-C₆H₃); 129.26 (p-C₆H₂Pr₂Bu^t); 137.37 (i-

- (16) (a) Schiemenz, B.; Power, P. P. *Angew. Chem., Int. Ed.* **1996**, *35*, 2150. (b) Schiemenz, B.; Power, P. P. *Organometallics* **1996**, *15*, 958.
- (17) Hardman, N. J.; Wright, R. J.; Phillips, A. D.; Power, P. P. *J. Am. Chem. Soc.* **2003**, *125*, 2667.
- (18) (a) Gilman, H.; Smith, C. L. *J. Organomet. Chem.* **1967**, *8*, 245. (b) Gutekunst, G.; Brook, A. G. *J. Organomet. Chem.* **1982**, *225*, 1. (c) Heine, A.; Herbst-Irmer, R.; Sheldrick, G. M.; Stalke, D. *Inorg. Chem.* **1993**, *32*, 2694.
- (19) (a) The ²⁰⁷Pb NMR spectra of **3–7** in C₆D₆ were externally referenced to Pb(NO₃)₂. The ²⁰⁷Pb chemical shift was converted to the Me₄Pb standard by adding 2961 ppm to the value obtained using Pb(NO₃)₂. Thus, the ²⁰⁷Pb chemical shifts for **3**, **4**, **5**, **6**, and **7** are 5777, 4314, 5296, 5589, and 7784 relative to Pb(NO₃)₂, but are 8738, 7275, 8257, 8550, and 10745 relative to PbMe₄. The data given in the Experimental Section and Table 3 have been corrected to refer to PbMe₄. (b) Marsmann, H. C. In *Chemistry of Organic Germanium, Tin and Lead Compounds*; Rappoport, Z., Ed.; Wiley: Chichester, 2002; Vol. 2, Part 1, Chapter 6. (c) Wrackmeyer, B.; Horchler, K. *Annu. Rep. NMR Spectrosc.* **1989**, *22*, 249.

$C_6H_2Pr_2Bu^i$); 146.38 (o- C_6H_3); 148.61 (o- $C_6H_2Pr_2Bu^i$); 150.75 (p- C_6H_3); 289.92 (i- C_6H_3). UV-vis (hexane): λ_{max} 417.0 nm, ϵ 760 $M^{-1} cm^{-1}$.

{Pb(CH₃ArPr₂)₂}, 3. Compound **1** (2.19 g, 0.80 mmol) was dissolved in diethyl ether (45 mL) and cooled to ca. $-30^\circ C$. CH₃MgBr (1.17 mL, 3.0 M in Et₂O) was added via syringe. The solution was allowed to warm to room temperature and stirred for 3 h, during which time the solution became deep red. The diethyl ether was removed under reduced pressure, and the red solid was extracted with hexanes (60 mL) and filtered through Celite. The filtrate was placed in a ca. $-20^\circ C$ freezer. Dichroic, red-green crystals of **2** were obtained upon storage for 2 days. Yield: 0.64 g, 65%. Mp: 210–214 $^\circ C$. Anal. Calcd for C₃₁H₄₀Pb: C, 60.01; H, 6.51. Found: C, 60.81; H, 6.92. ¹H NMR (C₆D₆): δ 0.10 (s, 3H, CH₃); 1.08 (d, 12H, o-CH(CH₃)₂) ³J_{HH} = 6.90 Hz; 1.31 (d, 12H, o-CH(CH₃)₂) ³J_{HH} = 6.90 Hz; 3.30 (sept, 4H, o-CH(CH₃)₂) ³J_{HH} = 6.90 Hz; 7.13 (d, 4H, m- $C_6H_3Pr_2$) ³J_{HH} = 6.75 Hz; 7.20 (t, 2H, p- $C_6H_3Pr_2$) ³J_{HH} = 6.75 Hz; 7.44 (t, 1H, p- C_6H_3) ³J_{HH} = 7.50 Hz; 7.75 (d, 2H, m- C_6H_3) ³J_{HH} = 7.20 Hz. ¹³C{¹H} NMR (C₆D₆): δ 1.59 (Pb-CH₃); 23.48 (o-CH(CH₃)₂); 26.48 (o-CH(CH₃)₂); 30.73 (o-CH(CH₃)₂); 123.41 (m- $C_6H_3Pr_2$); 125.70 (p- C_6H_3); 128.51 (o- C_6H_3); 136.22 (i- $C_6H_3Pr_2$); 137.29 (m- C_6H_3); 145.46 (o- $C_6H_3Pr_2$); 147.10 (p- $C_6H_3Pr_2$); 256.41 (i- C_6H_3). ²⁰⁷Pb{¹H} NMR (C₆D₆): δ 8738. UV-vis (hexane): λ_{max} 468.0 nm, ϵ 3180 $M^{-1} cm^{-1}$; 343 nm, ϵ 870 $M^{-1} cm^{-1}$.

Pb(C₆H₄-4-Buⁱ)ArPr₂, 4. A freshly prepared solution of 4-*tert*-butyl phenylmagnesium bromide (2.20 mL, 1.18 mmol, 0.54 M in THF) was added to a rapidly stirred solution of **1** (0.727 g, 0.53 mmol) in THF (40 mL) with cooling to ca. $0^\circ C$ in an ice bath. The reaction mixture became a red color and was allowed to warm to room temperature and stirred overnight. The THF was removed under reduced pressure and extracted with toluene (50 mL). The solution was filtered through Celite, concentrated, and stored in a ca. $-20^\circ C$ freezer to give orange crystals of **4**. Yield: 0.548, 70%. Mp: 100–102 $^\circ C$. ¹H NMR (C₆D₆): δ 1.082 (d, 12H, o-CH(CH₃)₂) ³J_{HH} = 6.90 Hz; 1.09 (d, 12H, o-CH(CH₃)₂) ³J_{HH} = 6.90 Hz; 1.25 (s, 9H, C(CH₃)₃); 3.36 (sept, 4H, o-CH(CH₃)₂) ³J_{HH} = 6.90 Hz; 7.06 (d, 4H, m- $C_6H_3Pr_2$) ³J_{HH} = 6.50 Hz; 7.17 (t, 2H, p- $C_6H_3Pr_2$) ³J_{HH} = 6.50 Hz; 7.47 (t, 1H, p- C_6H_3) ³J_{HH} = 7.80 Hz; 7.76 (d, 2H, o- C_6H_4) ³J_{HH} = 8.10 Hz; 7.89 (d, 2H, m- C_6H_3) ³J_{HH} = 7.80 Hz; 8.78 (d, 2H, m- C_6H_4) ³J_{HH} = 8.10 Hz. ¹³C{¹H} NMR (C₆D₆): δ 1.37 (C(CH₃)₃); 23.13 (o-CH(CH₃)₂); 26.83 (o-CH(CH₃)₂); 31.02 (o-CH(CH₃)₂); 31.42 (C(CH₃)₃); 123.49 (m- $C_6H_3Pr_2$); 124.74 (p- $C_6H_3Pr_2$); 128.83 (o- C_6H_3); 129.80 (o- $C_6H_4Bu^i$); 136.54 (i- $C_6H_3Pr_2$); 137.52 (m- $C_6H_4Bu^i$); 145.93 (o- $C_6H_3Pr_2$); 147.49 (p- $C_6H_3Pr_2$); 150.17 (p- $C_6H_4Bu^i$); 260.26 (i- $C_6H_4Bu^i$); 276.16 (i- C_6H_3). ²⁰⁷Pb{¹H} NMR (C₆D₆): 7275. UV-vis (hexane): λ_{max} 462 nm, ϵ 1020 $M^{-1} cm^{-1}$.

Pb(Buⁱ)ArPr₂, 5. In a manner similar to **3**, a THF solution of BuⁱMgCl (0.79 mL, 1.25 mmol, 20 wt % in THF) was added to a solution of **1** (0.717 g, 0.26 mmol) in diethyl ether (25 mL) at ca. $0^\circ C$ with constant stirring. Workup was as described for **3** and afforded **5** as dark purple crystals. Yield: 0.434 g, 63%. Mp: 115–118 $^\circ C$. Anal. Calcd for C₃₄H₄₆Pb: C, 61.69; H, 7.01. Found: C, 61.73; H, 7.47. ¹H NMR (C₆D₆): δ 1.064 (d, 12H, o-CH(CH₃)₂) ³J_{HH} = 6.90 Hz; 1.365 (d, 12H, o-CH(CH₃)₂) ³J_{HH} = 6.90 Hz; 3.263 (sept, 4H, o-CH(CH₃)₂) ³J_{HH} = 6.90 Hz; 3.831 (s, 9H, C(CH₃)₃); 7.133 (d, 4H, m- $C_6H_3Pr_2$) ³J_{HH} = 3.90 Hz; 7.182 (t, 4H, p- $C_6H_3Pr_2$) ³J_{HH} = 3.90 Hz; 7.441 (t, 1H, p- C_6H_3) ³J_{HH} = 7.80 Hz; 7.825 (d, 2H, m- C_6H_3) ³J_{HH} = 7.80 Hz. ¹³C{¹H} NMR (C₆D₆): δ 23.44 (o-CH(CH₃)₂); 24.73 (C(CH₃)₃); 26.16 (o-CH(CH₃)₂); 31.05 (o-CH(CH₃)₂); 123.68 (m- $C_6H_3Pr_2$); 124.40 (p- C_6H_3); 137.24 (m- C_6H_3); 137.89 (i- $C_6H_3Pr_2$); 145.49 (o- $C_6H_3Pr_2$); 147.30 (p- $C_6H_3Pr_2$);

173.71 (o- C_6H_3); 262.70 (i- C_6H_3). ²⁰⁷Pb{¹H} NMR (C₆D₆): 8257. UV-vis (hexane): λ_{max} 581.0 nm, ϵ 740 $M^{-1} cm^{-1}$.

Pb(CH₂C₆H₄-4-Prⁱ)ArPr₂, 6. Compound **6** was synthesized in a manner similar to **4** with use of a freshly prepared 4-isopropylbenzylmagnesium bromide solution (5.75 mL, 0.189 M in THF) and {Pb(μ -Br)ArPr₂}₂ (0.808 g, 0.525 mmol, 20 mL Et₂O). The reaction mixture became a deep purple color. The mixture was allowed to warm to room temperature and stirred for 8 h. The volatile solvent was removed under reduced pressure, and the remaining residue was extracted with hexanes and filtered through Celite. The solvent volume was reduced to incipient crystallization and cooled in a ca. $-20^\circ C$ freezer to afford **6** as dark red crystals. Yield: 0.381 g, 46.5%. Mp: 176–178 $^\circ C$. Anal. Calcd for C₄₆H₆₂Pb: C, 67.20; H, 7.60. Found: C, 67.91; H, 7.25. ¹H NMR (C₆D₆): δ 1.13 (d, 12H, p-CH(CH₃)₂) ³J_{HH} = 6.80 Hz; 1.16 (d, 6H, -CH₂-(C₆H₄)-CH(CH₃)₂) ³J_{HH} = 6.40 Hz; 1.26 (d, 12H, o-CH(CH₃)₂) ³J_{HH} = 6.80 Hz; 1.38 (d, 12H, o-CH(CH₃)₂) ³J_{HH} = 6.80 Hz; 1.55 (s, 2H, -CH₂-(C₆H₄)-CH(CH₃)₂); 2.84 (sept, 2H, p-CH(CH₃)₂) ³J_{HH} = 6.80; 2.91 (sept, 2H, -CH₂-(C₆H₄)-CH(CH₃)₂) ³J_{HH} = 6.40; 3.33 (sept, 4H, o-CH(CH₃)₂) ³J_{HH} = 6.80 Hz; 6.02 (d, 2H, m-(C₆H₄)-CH(CH₃)₂) ³J_{HH} = 8.40 Hz; 7.17 (d, 2H, o-(C₆H₄)-CH(CH₃)₂) ³J_{HH} = 8.40 Hz; 7.23 (s, 4H, m- $C_6H_2Pr_3$); 7.44 (t, 1H, p- C_6H_3) ³J_{HH} = 7.60 Hz; 7.44 (d, 2H, m- C_6H_3) ³J_{HH} = 7.60 Hz. ¹³C{¹H} NMR (C₆D₆): δ 1.37 (CH₂); 23.68 (o-CH(CH₃)₂); 24.41 (o-CH(CH₃)₂); 24.56 (CH₂(C₆H₄)CH(CH₃)₂); 26.57 (p-CH(CH₃)₂); 30.88 (o-CH(CH₃)₂); 33.03 ((C₆H₄)CH(CH₃)₂); 34.780 (p-CH(CH₃)₂); 120.76 (o- C_6H_4); 121.59 (m- $C_6H_2Pr_3$); 124.96 (o- $C_6H_2Pr_3$); 125.05 (m- C_6H_4); 128.75 (p- C_6H_3); 135.66 (i- $C_6H_2Pr_3$); 135.95 (i- C_6H_4); 136.93 (m- C_6H_3); 145.11 (p- C_6H_4); 145.86 (o- C_6H_3); 147.20 (p- $C_6H_2Pr_3$); 263.68 (i- C_6H_3). ²⁰⁷Pb{¹H} NMR (C₆D₆): 8550. UV-vis (hexane): λ_{max} 556.0 nm, ϵ 860 $M^{-1} cm^{-1}$; 391.0 nm, ϵ 710 $M^{-1} cm^{-1}$.

Pb{Si(SiMe₃)₃}ArPr₂, 7. {Pb(μ -Br)ArPr₂}₂ (0.769 g, 0.500 mmol, 25 mL Et₂O) was cooled to $-78^\circ C$ and added to a solution of Li{Si(SiMe₃)₃} (0.463 g, 1 mmol, 10 mL Et₂O). The mixture was allowed to warm to room temperature and stirred overnight. The volatile solvent was removed under reduced pressure, and the remaining residue was extracted with hexanes (50 mL) and filtered through Celite. The solvent volume was reduced to incipient crystallization to afford teal crystals of **7**. Yield: 0.52 g, 55.5%. Mp: 120–122 $^\circ C$. ¹H NMR (C₆D₆): δ 0.228 (Si(Si(CH₃)₃)); 1.111 (d, 12H, o-CH(CH₃)₂) ³J_{HH} = 6.80 Hz; 1.234 (d, 12H, o-CH(CH₃)₂) ³J_{HH} = 6.80 Hz; 1.418 (d, 12H, p-CH(CH₃)₂) ³J_{HH} = 6.80 Hz; 2.778 (sept, 2H, p-CH(CH₃)₂) ³J_{HH} = 6.80; 3.308 (sept., 4H, o-CH(CH₃)₂) ³J_{HH} = 6.80 Hz; 7.074 (s, 4H, m- $C_6H_2Pr_3$); 7.315 (t, 1H, p- C_6H_3) ³J_{HH} = 7.50 Hz; 7.769 (d, 2H, m- C_6H_3) ³J_{HH} = 7.50 Hz. ¹³C{¹H} NMR (C₆D₆): δ 8.359 (Si(SiCH₃)₃); 24.448 (o-CH(CH₃)₂); 24.757 (o-CH(CH₃)₂); 26.525 (p-CH(CH₃)₂); 31.416 (o-CH(CH₃)₂); 34.755 (p-CH(CH₃)₂); 120.723 (m- $C_6H_2Pr_3$); 122.210 (o- $C_6H_2Pr_3$); 128.315 (p- C_6H_3); 134.348 (i- $C_6H_2Pr_3$); 139.424 (m- C_6H_3); 146.990 (p- C_6H_3); 147.362 (o- C_6H_3); 148.610 (p- $C_6H_2Pr_3$); 263.68 (i- C_6H_3). ²⁹Si NMR (C₆D₆): δ 3.89 (Si(SiMe₃)); 185.32 (Si(SiMe₃)₃). ²⁰⁷Pb{¹H} NMR (C₆D₆): δ 10745. IR (Nujol): $\tilde{\nu}$ 1605 w, 1565 vw, 1365 w, 1240 m, 945 vw, 830 vs, 720 w, 680 m, 615 m, 245m. UV-vis (hexane): λ_{max} 725 nm, ϵ 260 $M^{-1} cm^{-1}$; 415 nm, ϵ 270 $M^{-1} cm^{-1}$.

Crystallographic Studies. Crystals of **1–7** were covered with hydrocarbon oil under a rapid flow of argon, mounted on a glass fiber attached to a copper pin, and placed in a N₂ cold stream on the diffractometer. X-ray data were collected on a Bruker SMART 1000 diffractometer at 90(2) K with use of Mo K α radiation (λ =

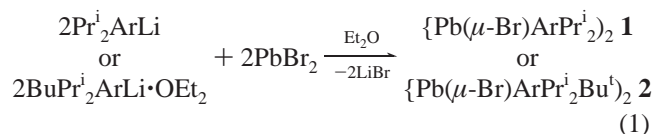
Table 1. Crystallographic Data for Compounds 1–7

	1	2·2PhMe	3	4·0.25n-hexane	5	6	7·0.5n-hexane
formula	C ₆₀ H ₇₄ Br ₂ Pb ₂	C ₉₀ H ₁₂₂ Br ₂ Pb ₂	C ₆₂ H ₈₀ Pb ₂	C _{41.5} H _{53.5} Pb	C ₃₄ H ₄₆ Pb	C ₄₆ H ₆₂ Pb	C ₄₈ H ₈₃ PbSi ₄
fw	1369.40	1778.08	1239.64	759.53	661.90	822.15	979.69
color, habit	orange, prism	yellow, needles	dichroic	red, needles	royal blue, needles	red, needles	light blue, blocks
cryst syst	monoclinic	triclinic	orthorhombic	triclinic	monoclinic	monoclinic	monoclinic
space group	<i>P</i> 2 ₁ / <i>n</i>	<i>P</i> 1	<i>Pbca</i>	<i>P</i> 1	<i>P</i> 2 ₁ / <i>n</i>	<i>P</i> 2 ₁ / <i>n</i>	<i>P</i> 2 ₁ / <i>c</i>
<i>a</i> , Å	13.3164(2)	14.230(2)	15.668(2)	13.477(3)	9.666(2)	8.0428(5)	19.6824(12)
<i>b</i> , Å	14.1792(2)	14.791(3)	17.285(2)	16.148(3)	9.567(2)	18.6486	15.9100(8)
<i>c</i> , Å	14.6144(2)	20.433(4)	20.011(3)	19.017(4)	32.913(7)	27.0344	16.9291(10)
α, deg	90.0	100.245(7)	90.0	105.856(3)	90.0	90.0	90.0
β, deg	97.538(8)	94.306(6)	90.0	106.890(3)	95.306(4)	96.516(3)	101.041(3)
γ, deg	90.0	97.848(7)	90.0	101.503(3)	90.0	90.0	90.0
<i>V</i> , Å ³	2735.6(6)	4170.8(13)	5419.4(12)	3630.4(13)	3030.6(11)	4028.6(5)	5203.2(5)
<i>Z</i>	2	2	4	4	4	4	4
<i>d</i> _{calc} , Mg/m ³	1.662	1.416	1.519	1.389	1.451	1.356	1.251
θ range, deg	1.95–26.00	1.42–27.5	2.03–25.25	1.80–25.35	2.30–30.00	1.33–27.5	1.77–25.25
μ, mm ⁻¹	7.643	5.031	6.241	4.673	5.586	4.217	3.363
obsd data <i>I</i> > 2σ(<i>I</i>)	4780	13702	2550	9825	5618	7757	7625
R1 (obsd data)	0.0209	0.0343	0.0321	0.0385	0.0595	0.0276	0.0331
wR2 (all data)	0.0560	0.0869	0.0987	0.0997	0.1300	0.0677	0.0644

0.71073 Å). Absorption corrections were applied using SADABS.²⁰ The structures were solved with use of direct methods or the Patterson option in SHELXS²¹ and refined by the full-matrix least-squares procedure in SHELXL.²¹ All non-hydrogen atoms were refined anisotropically, while hydrogens were placed at calculated positions and included in the refinement by using a riding model. Some details of the data collection and refinement are given in Table 1. Further details are in the Supporting Information.

Results and Discussion

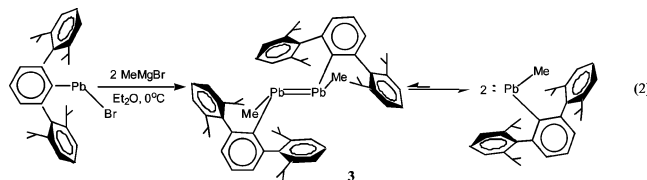
Synthesis and Spectroscopy. The aryl lead halides, {Pb(*μ*-Br)ArPr₂}₂ (**1**), and the related species {Pb(*μ*-Br)ArPr₂-Bu^{*i*}}₂ (**2**) were synthesized by treating a diethyl ether suspension of lead(II) bromide with a diethyl ether solution of a stoichiometric quantity of ArPr₂Li or Bu^{*i*}Pr₂ArLi·OEt₂ (eq 1).



Orange crystals of **1** or **2** were isolated in good yield, and these were stable up to their melting points of 201 or 256 °C, respectively. Both the ¹H and ¹³C NMR spectra of **1** and **2** were easily obtained in C₆D₆, but no ²⁰⁷Pb NMR signal could be observed. It is possible that the difficulty in detecting this signal is associated with the large anisotropies expected for the components of the chemical shift tensor. Also, the presence of the quadrupolar nuclei ⁷⁹Br and ⁸¹Br linked to the lead atom could be a factor in broadening the ²⁰⁷Pb NMR signal beyond the limit of observation. The difficulty associated with obtaining a ²⁰⁷Pb NMR signal for **1** and **2** is consistent with the previous reports of Eaborn, Smith, and co-workers²² on the organolead chlorides

{Pb(*μ*-Cl)C(SiMe₃)₂(SiMe₂OMe)}₂, [Pb(*μ*-Cl){C(SiMe₃-Ph)₃}₂], and [Pb(*μ*-Cl){C(SiMe₃)₃}₃] as well as our previous work on the related organolead bromides {Pb(*μ*-Br)ArPr₂}₂¹⁴ and ArPr₂Pb(py)Br.¹⁴ The reactions of compound **2** were not further pursued due to the tendency of the products to display crystallographic problems and the fact the bulky ArPr₂Bu^{*i*} ligand was unlikely to permit a Pb–Pb bond to be observed.

The plumbylene dimer, **3**, was synthesized by reaction of **1** with 1 equiv of MeMgBr. The reaction proceeded smoothly to give a moderate yield of the product as thermally robust, red crystals. The ²⁰⁷Pb NMR spectrum for **3** displayed a signal at 8738 ppm, which is very similar to that reported (8750 ppm) for Pb(Me)ArPr₂¹⁴ for which a monomeric structure has been already established. This indicates that dissociation to monomers is essentially complete in solution at room temperature.²³ In addition, the UV–vis spectrum of **3** displayed absorption maxima at 343 and 468 nm, and these values are very similar to those of Pb(Me)ArPr₂, which has maxima at 332 and 466 nm.



The weakly dimerized **4** and the monomers **5**–**7** were synthesized by the reaction of the aryl lead bromide with

(23) The chemical shifts reported here for compounds **3**–**7** are consistent with those previously reported for two coordinate organolead compounds.^{19b,c} An increase in the coordination number of lead from two to three, which occurs upon association, is expected to result in a large chemical shift change (>1000 ppm upfield) such as that observed when the lead carbene adduct (NN)PbC(NN) (NN = 1,2-(Bu^{*i*}CH₂N)₂C₆H₄) dissociates in solution.^{23a} The consistency of the shifts observed for **3**–**7** with those previously reported for two-coordinate species led us to conclude that **3**–**7** were also two-coordinate in solution at room temperature. The relatively low solubility of **3** and **6** has so far prevented us from investigating the monomer–dimer equilibrium for these species by VT ²⁰⁷Pb NMR spectroscopy. (a) Gehrus, B.; Hitchcock, P. B.; Lappert, M. F. *Dalton Trans.* **2000**, 3094.

(20) SADABS: Area-Detection Absorption Corrections; Bruker AXS Inc.: Madison, WI, 1996.

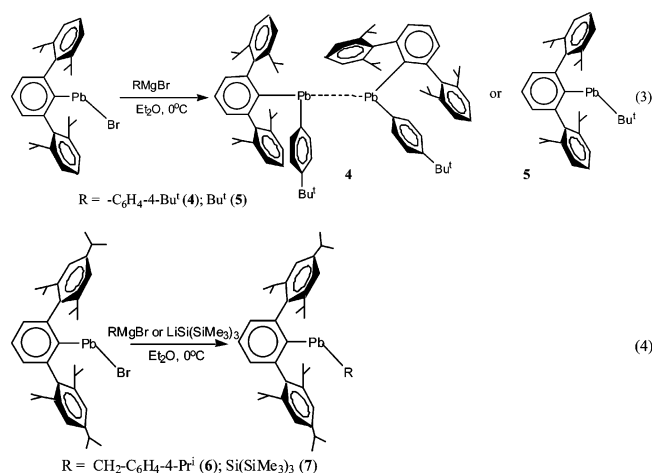
(21) SHELXTL, PC version 5.03; Bruker AXS Inc.: Madison, WI, 1994.

(22) Eaborn, C.; Hitchcock, P. B.; Smith, J. D.; Soezerli, S. E. *Organometallics* **1997**, *16*, 5653.

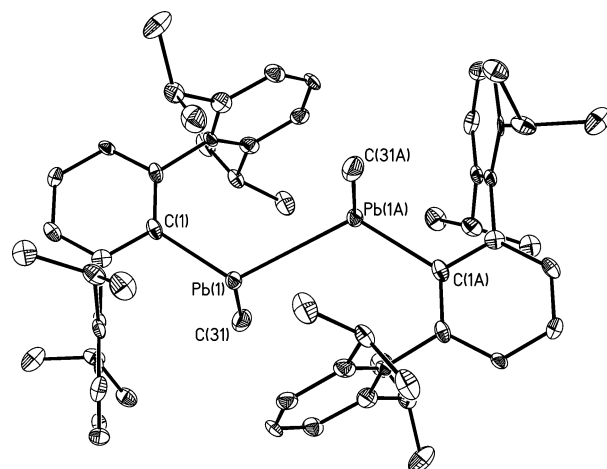
Table 2. Selected Bond Distances (Å) and Bond Angles (deg) for Compounds 1–7

1		2		3		4	
Pb(1)–C(1)	2.322(3)	Pb(1)–C(1)	2.338(5)	Pb(1)–C(31)	2.280(6)	Pb(1)–C(31)	2.275(6)
Pb(1)–Br(1)	2.8125(5)	Pb(1)–Br(1)	2.9202(7)	Pb(1)–C(1)	2.318(6)	Pb(1)–C(1)	2.311(5)
Pb(1)–Br(1A)	3.0346(5)	Pb(1)–Br(2)	2.9191(7)	Pb(1)–Pb(1A)	3.1601(6)	Pb(1)–Pb(2)	3.927(1)
C(1)–Pb(1)–Br(1)	91.23(8)	Pb(2)–C(39)	2.346(4)	C(1)–C(6)	1.386(8)	C(31)–Pb(1)–C(1)	94.53(19)
C(1)–Pb(1)–Br(1A)	109.64(9)	Pb(2)–Br(2)	2.8713(7)	C(31)–Pb(1)–C(1)	91.8(2)	C(6)–C(1)–C(2)	120.0(5)
Br(1)–Pb(1)–Br(1A)	89.014(10)	Pb(2)–Br(1)	2.9419(7)	C(31)–Pb(1)–Pb(1A)	109.35(16)	C(6)–C(1)–Pb(1)	124.3(4)
Pb(1)–Br(1)–Pb(1A)	90.986(10)	C(1)–Pb(1)–Br(2)	108.02(11)	C(1)–Pb(1)–Pb(1A)	121.51(14)	C(2)–C(1)–Pb(1)	115.1(4)
C(2)–C(1)–C(6)	119.5(3)	C(1)–Pb(1)–Br(1)	97.17(11)	C(6)–C(1)–C(2)	119.8(5)		
C(2)–C(1)–Pb(1)	109.0(2)	Br(2)–Pb(1)–Br(1)	86.75(2)	C(6)–C(1)–Pb(1)	125.9(4)		
C(6)–C(1)–Pb(1)	131.4(3)	C(39)–Pb(2)–Br(2)	106.82(11)	C(2)–C(1)–Pb(1)	114.2(4)		
C(3)–C(2)–C(1)	120.9(3)	C(39)–Pb(2)–Br(1)	98.41(10)	C(3)–C(2)–C(1)	119.2(5)		
		Br(2)–Pb(2)–Br(1)	87.22(2)				
		Pb(1)–Br(1)–Pb(2)	92.26(2)				
		Pb(2)–Br(2)–Pb(1)	93.74(2)				
		C(2)–C(1)–C(6)	118.6(4)				
		C(2)–C(1)–Pb(2)	108.6(3)				
		C(6)–C(1)–Pb(1)	132.7(3)				
5		6		7			
Pb(1)–C(31)	2.301(7)	Pb(1)–C(1)	2.294(3)	C(1)–Pb(1)	2.296(3)		
Pb(1)–C(1)	2.301(6)	Pb(1)–C(37)	2.317(3)	Pb(1)–Si(1)	2.7230(11)		
C(31)–Pb(1)–C(1)	102.5(2)	C(1)–Pb(1)–C(37)	97.64(11)	C(1)–Pb(1)–Si(1)	110.82(9)		
C(2)–C(1)–C(6)	119.3(6)	C(6)–C(1)–C(2)	120.0(2)				
C(2)–C(1)–Pb(1)	122.8(4)	C(6)–C(1)–Pb(1)	120.14(19)				
C(6)–C(1)–Pb(1)	116.6(4)	C(2)–C(1)–Pb(1)	118.28(19)				
C(3)–C(2)–C(1)	119.6(6)						

the Grignard reagents, 4-^tBuC₆H₄MgBr, ^tBuMgBr, 4-ⁱPr-C₆H₄-CH₂-MgBr, or the lithium reagent, LiSi(SiMe₃)₃, as shown in eqs 3 and 4:



Pb(C₆H₄-4-Bu^t)ArPr₂, **4**, was prepared as red-orange crystals by the addition of 4-*tert*-butyl phenylmagnesium bromide to a rapidly stirred solution of **1**. The spectroscopic data obtained are very similar to those found in Pb(Ph)ArPr₃.¹⁴ For **4**, the maximum absorption was at 462 nm, cf. 460 nm for Pb(Ph)ArPr₃.¹⁴ Compound **5** was obtained as royal blue X-ray quality crystals. The ²⁰⁷Pb NMR signal and the UV–vis spectrum were consistent with the monomeric Pb(Bu^t)ArPr₃. The ²⁰⁷Pb NMR signal at 8257 ppm is close to that reported for Pb(Bu^t)ArPr₃ (8756 ppm). The UV–vis spectrum of **5** displays a maximum at 581 nm, cf. 571 nm for Pb(Bu^t)ArPr₃. Similarly, the reaction of 4-isopropyl-benzylmagnesium bromide with a rapidly stirred solution of {Pb-(*μ*-Br)ArPr₃}₂ in Et₂O yielded **6**, Pb(CH₂C₆H₄-4-Prⁱ)ArPr₃,

**Figure 1.** Thermal ellipsoid plot of **3**. H atoms are not shown for clarity. Selected bond distances and angles are given in Table 2.

in moderate yield. Its ²⁰⁷Pb NMR chemical shift, 8559 ppm, is further downfield than the 5067 ppm value observed for the previously reported benzyl derivative Pb(CH₂CMe₂C₆H₃-Bu^t)₂Mes*,^{9b} where Mes* = 2,4,6-Bu^t-C₆H₂. The upfield chemical shift may be attributed to the increased coordination in the latter compound, where the *tert*-butyl groups assist in the stabilization of the Pb center through CH–Pb interactions. The UV–vis absorption maxima for **6** (556 nm) resembles the other *m*-terphenyl lead alkyl complexes. The silyl substituted plumbylene, Pb{Si(SiMe₃)₃}ArPr₃, **7**, was synthesized by the reaction of {Pb-(*μ*-Br)ArPr₃}₂ with 1 equiv of LiSi(SiMe₃)₃. The reaction yielded X-ray quality, teal crystals. The ²⁰⁷Pb NMR signal observed for **7** was similar to that for the previously reported Pb{Si(SiMe₃)₃}ArMe₃,²⁴ where ArMe₃ = -C₆H₃-2,6-(C₆H₂-2,4,6-Me₃)₂.

Table 3. Spectroscopic and Structural Parameters for Selected Diorganolead Compounds Including **1–7**

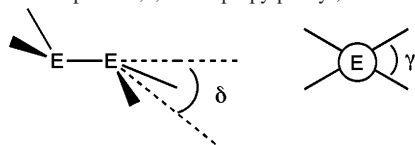
	Pb–C (Å)	Pb angle (deg)	²⁰⁷ Pb NMR (δ)	UV–vis (nm)	ref
[Pb(Me)ArPr ⁱ ₂] ₂ (3)	2.318(6)	91.8(2)	8738	470; 340	this work
Pb(C ₆ H ₄ -4-Bu ^l)ArPr ⁱ ₂ (4)	2.311(5), 2.275(6)	94.53(19)	7275	462	this work
Pb(Bu ^l)ArPr ⁱ ₂ (5)	2.301(6)	102.5(2)	8257	520	this work
Pb{CH ₂ C ₆ H ₄ -4-Pr ⁱ }ArPr ⁱ ₃ (6)	2.294(3)	97.64(11)	8550	860; 390	this work
Pb{Si(SiMe ₃) ₃ }ArPr ⁱ ₃ (7)	2.296(4)	110.8(3)	10745	730; 420	this work
Pb(Me)ArPr ⁱ ₃	2.272(9), 2.274(15)	101.4(4)	8750	446; 332	14
Pb(Ph)ArPr ⁱ ₃	2.321(3), 2.264(3)	95.64(11)	7987	460	14
Pb(Bu ^l)ArPr ⁱ ₃	2.289(11), 2.274(15)	100.5(5)	8556	570	14
Pb{CH ₂ CMe ₂ C ₆ H ₃ Bu ^t } ₂ Mes ^{*a}	2.344(9), 2.476(14)	94.8	5067	406	9b
Pb{Si(SiMe ₃) ₃ }ArMe ₃	2.290(4)	109.17(11)	10510	720; 399	24
Pb[C ₆ H ₂ -2,4,6-{CH(SiMe ₃) ₂ }] ₃	2.33(1)	116.3(7)	8971	610	27
Pb{ArMe ₃ } ₂	2.334(12)	114.5(6)	8844	526	26
{Pb(<i>μ</i> -Br)ArPr ⁱ ₂ Bu ^l } ₂ (2)	2.335(3)	97.24(19), 108.08(19)		420	this work
{Pb(<i>μ</i> -Br)ArPr ⁱ ₃ } ₂	2.317(62)	95.4(3), 98.0(3)		420	14
{Pb(<i>μ</i> -Br)ArPr ⁱ ₂ } ₂ (1)	2.322(3)	91.23(8), 109.64(9)		420	this work
[Pb(C ₆ H ₅ CH ₃)ArPr ⁱ ₃][MeB(C ₆ F ₅) ₃]	2.250(7)	127.0(1)	8974	430	28

^a Mes* = –C₆H₂-2,4,6-Bu^t₃; ArMe₃ = –C₆H₃-2,6-(2,4,6-Me₃C₆H₂)₂.

Table 4. Structural and Spectroscopic Parameters of Diplumbenes Including **3** and **4**^a

	Pb=Pb (Å)	Pb–Ar or Pb–R (Å)	Ar–Pb–R (deg)	²⁰⁷ Pb NMR (δ)	UV–vis (nm)	δ (deg)	γ (deg)	ref
{PbTrip ₂ } ₂	3.0515(3)	2.288(5), 2.293(5)	97.8(2), 102.3(2)		541, 385, 321	43.9, 51.2		9c
[Mes ₂ Pb{2MgBr ₂ (THF) ₄ }] ₂	3.3549(6)	2.322(5), 2.304(6)	97.4			71.0	0	9d
[Pb{Si(SiMe ₃) ₃ }Mes] ₂	2.903(11)	2.314(10), 2.681(3) Si	102.5(3)			61.0	0	8
[Pb{Si(SiMe ₃) ₃ }Trip] ₂	2.899(5)	2.296(4), 2.717(1) Si	108.8(1)		770, 591, 350	42.7	0	9e
[Pb{Si(SiMe ₃) ₃ }Ar ^F] ₂	3.537(1)	2.369(7), 2.705(2) Si	96.7(2)		1025, 586	40.8	0	9a
[Pb{Si(SiMe ₃) ₃ }Bmp] ₂	3.33695(11)	2.37(2), 2.709(4) Si	106.0(3)	7545	610, 341, 303	46.5	0	9b
{Pb(Me)ArPr ⁱ ₂ } ₂ (3)	3.1601(6)	2.318(6), 2.289(6)	91.8(2)	8738	468, 343	51.8	0	this work
{Pb(C ₆ H ₄ -4-Bu ^l)ArPr ⁱ ₂ } ₂ (4)	3.947(1)	2.275(6), 2.311(5)	94.53(19)	7275		35.5, 3.9	74.2	this work
[Pb{CH(SiMe ₃) ₂ }] ₂	4.129			9112		34.2		9b

^a Trip = 2,4,6-triisopropylphenyl; Mes = 2,4,6-trimethylphenyl; Hyp = Si(SiMe₃)₃; Ar^F = C₆H₂-2,4,6-(CF₃)₃; Bmp = 2-Bu^l-4,5,6-Me₃C₆H.



Structures. In both **1** and **2**, the molecules are dimerized through bridging of the lead centers by two bromides. The bond distances and angles resemble those already reported for {Pb(*μ*-Br)ArPrⁱ₃}₂,¹⁴ and for the three compounds, the Pb–C and Pb–Br distances span the narrow ranges 2.322(3)–2.340(7) and 2.7841(16)–3.034(5) Å, respectively. The X-ray structure of the “diplumbene” **3** shows that it has a trans-pyramidal structure as illustrated in Figure 1 with a Pb–Pb distance 3.1601(6) Å and an out-of-plane angle of 51.8°. These structural parameters can be compared with those of the previously reported “diplumbenes” in Table 4. The Pb–Pb bond length lies in the middle of the previously known range (2.899(5)–3.537(1) Å); however, it should be noted that even the shortest of these distances does not imply strong Pb–Pb interaction or that the complex will remain dimeric in solution. The ²⁰⁷Pb NMR spectrum clearly shows

that **3** is completely dissociated in benzene,²³ and it may be concluded that the Pb–Pb bond in **3** is weak and a relatively small increase in crowding would be sufficient to dissociate the bond. This is what happens in the closely related species Pb(Me)ArPrⁱ₃,¹⁴ which remains monomeric in the solid state. The only difference between Pb(Me) and **3** is the absence of Prⁱ groups at the para positions of the flanking aryls in **3**. Inspection of the thermal ellipsoid plot of **3** clearly shows that if the para Prⁱ groups were present in the structure, they would cause steric interference between each other across the Pb–Pb bond which is sufficient to cause dissociation to monomers in the crystal phase as observed in Pb(Me). A similar relationship between monomeric and dimeric structures is observed when ArPrⁱ₂ and ArPrⁱ₃ ligands are employed in the neighboring group 13 element derivatives MArPrⁱ₃ and Prⁱ₂ArMMArPrⁱ₂ (M = In or Tl),²⁵ where their use allows weakly dimerized structures for Prⁱ₂ArMMArPrⁱ₂ to be observed,^{25c,d} whereas dissociated one-coordinate

(24) Klett, J.; Klinkhammer, K. W.; Niemeyer, M. *Chem.–Eur. J.* **1999**, *5*, 2531.

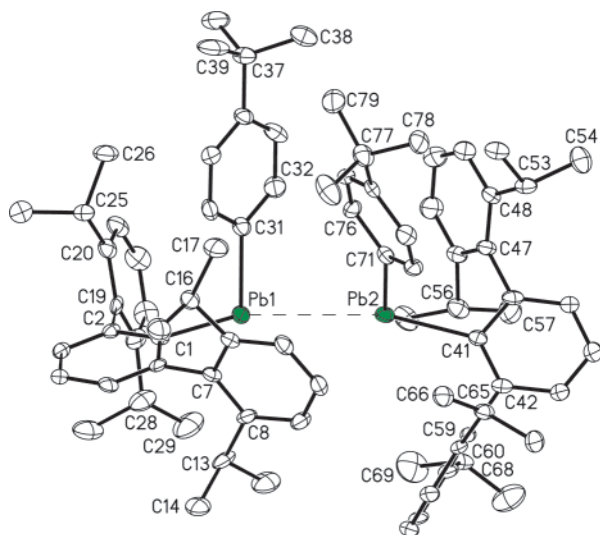


Figure 2. Thermal ellipsoid plot of **4**. H atoms are not shown for clarity. Selected bond distances and angles are given in Table 2.

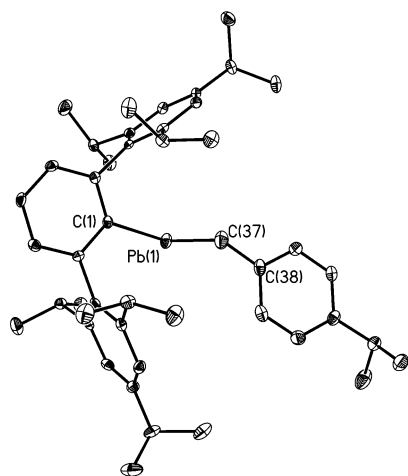


Figure 3. Thermal ellipsoid plot of **6**. H atoms are not shown for clarity. Selected bond distances and angles are given in Table 2.

monomeric structures are observed for $\text{MArPr}_3^{i,25a,b}$ in the solid state.

An almost parallel situation is observed in the case of the monomeric species $\text{Pb(Ph)ArPr}_3^{i,14}$ and the weakly dimerized **4**, which has a long Pb–Pb separation of 3.947(1) Å. Only $[\text{Pb}\{\text{CH}(\text{SiMe}_3)_2\}_2]_2^{9b}$ displays a longer Pb–Pb interaction of 4.129 Å for a diplumbene dimer. The thermal ellipsoid plot of **4** (Figure 2) shows that the *p-tert*-butyl groups on the phenyl substituents contribute to steric interference which may weaken the Pb–Pb bond. Unfortunately, attempts to grow crystals of Pb(Ph)ArPr_2^i to test this hypothesis were unsuccessful. Other features of the structures of **4** merit comment. In particular, it is notable that Pb(1) (35.5°) and Pb(2) (3.9°) possess different out-of-plane angles and the twist angle between the two lead coordination planes is 74.2°.

The latter parameter underlines the lack of any multiple character in the Pb–Pb bond. It seems probable that crystal packing forces could account for the observed Pb–Pb interaction as the packing arrangement for this structure appears to be influenced by parallel relationships between the aromatic substituents.

The structures **5–7** feature two-coordinate lead centers with a V-shaped geometry. For **5**, the Pb(1)–C(1) and the Pb(1)–C(31) distances are 2.301(6) and 2.301(7) Å, respectively. These distances are similar to those reported for $\text{Pb}(\text{Bu}^t)\text{ArPr}_3^{i,14}$ however, there is a lengthening of the Pb–C(ipso) bond and a shortening of the Pb–(Bu^t) bond in **5**. The X-ray crystallographic analysis of the benzylic derivative **6** (see Figure 3) revealed that the Pb–C(ipso) (2.294(3) Å) and Pb–C(benzyl) (2.317(3) Å) are considerably shorter than the corresponding distances in $\text{Pb}(\text{CH}_2\text{CMe}_2\text{C}_6\text{H}_3\text{-3,5-Bu}^t)\text{-Mes}^*$ isolated by Weidenbruch and co-workers,^{9b} where the Pb–C(ipso) length is 2.344(9) Å and the Pb–C(alkyl) bond is 2.476(14) Å. The extreme crowding in the Mes* derivative, which caused its rearrangement to $\text{Pb}(\text{CH}_2\text{CMe}_2\text{C}_6\text{H}_3\text{-3,5-Bu}^t)\text{Mes}^*$ in the first instance, accounts for the long Pb–C distances. For the silyl substituted plumbylene, **7**, the angle at the two-coordinate lead, 110.8(3)°, is just 1° wider than in $\text{Pb}\{\text{Si}(\text{SiMe}_3)_3\}\text{ArMe}_3$ despite the use of the larger substituent Ar*. The Pb–C bond and Pb–Si distances are 2.296(4) and 2.723 Å, respectively, which are also very similar to those in $\text{Pb}\{\text{Si}(\text{SiMe}_3)_3\}\text{ArMe}_3^{i,24}$.

Conclusion

The use of the terphenyl ligand ArPr_2^i which lacks para-Prⁱ groups on the flanking aryl rings has permitted examination of the weak Pb–Pb bonding in diplumbenes. In contrast to the corresponding ArPr_3^i derivatives which are monomeric in the solid state, the use of the slightly less crowding ArPr_2^i ligand permits weak Pb–Pb bonding to occur. Nonetheless, solution spectroscopic data for all diorganolead derivatives of the ArPr_2^i and ArPr_3^i ligands show that they are exclusively monomeric in solution. The behavior of these lead-(II) aryl derivatives, having simple methyl or phenyl groups as coligands, is in marked contrast to those of the corresponding tin(II) derivatives where disproportionation to tin(I)/tin(III) compounds is observed.²⁹

Acknowledgment. The authors would like to thank the National Science Foundation for financial support and Dr. P. Bruins and E. Rivera for useful discussions and technical assistance.

Supporting Information Available: Crystallographic data in CIF format. This material is available free of charge via the Internet at <http://pubs.acs.org>.

IC049174Y

(25) (a) Haubrich, S. T.; Power, P. P. *J. Am. Chem. Soc.* **1998**, *120*, 2202. (b) Niemeyer, M.; Power, P. P. *Angew. Chem., Int. Ed.* **1998**, *37*, 1277. (c) Wright, R. J.; Phillips, A. D.; Hardman, N. J.; Power, P. P. *J. Am. Chem. Soc.* **2002**, *124*, 8538. (d) Hardman, N. J.; Wright, R. J.; Phillips, A. D.; Power, P. P. *Angew. Chem., Int. Ed.* **2002**, *41*, 2842.

(26) Simons, R. S.; Pu, L. H.; Olmstead, M. M.; Power, P. P. *Organometallics* **1997**, *16*, 1920.
(27) Kano, N.; Shibata, K.; Tokitoh, N.; Okazaki, R. *Organometallics* **1999**, *18*, 2999.
(28) Hino, S.; Phillips, A. D.; Power, P. P. *Angew. Chem., Int. Ed.* **2004**, *43*, 2655.
(29) Phillips, A. D.; Hino, S.; Power, P. P. *J. Am. Chem. Soc.* **2003**, *125*, 7520–7521.